SINGLE-TREE FOREST INVENTORY USING LIDAR AND AERIAL IMAGES FOR 3D TREETOP POSITIONING, SPECIES RECOGNITION, HEIGHT AND CROWN WIDTH ESTIMATION

I. Korpela, B. Dahlin, H. Schäfer, E. Bruun, F. Haapaniemi, J. Honkasalo, S. Ilvesniemi, V. Kuutti, M. Linkosalmi, J. Mustonen, M. Salo, O. Suomi, H. Virtanen

Department of Forest Resource Management, POB 27, 00014 University of Helsinki, Finland – ilkka.korpela@helsinki.fi

Commission III

KEY WORDS: Allometry, Modeling, Mapping, Sampling, Photo-plot, Calibration, Multi-Scale, Matching, Template

ABSTRACT:

An entire single-tree remote sensing (STRS) system was developed and tested in an inventory of timber resources of a 56.8-hectare forest. A semi-automatic approach with operator intervention is used in the system and it solves the essential tasks of STRS: 3D treetop positioning, height estimation, species recognition, crown width estimation and the model-based allometric estimation of the stem diameter. Large-scale aerial imagery, an accurate DTM and semi-dense LiDAR data are required. The relatively low sampling density of the LiDAR, 6 points per m^2 here, was considered appropriate for crown width estimation, when the 3D treetop position, tree height estimation and species classification are done first using the images. LiDAR-based crown width estimation was done using crown modeling, in which parametric crown instances are iteratively fitted with the LiDAR data. Image-based 3D treetop positioning and crown width estimation rely on multi-scale template matching (MSTM). Species recognition was done by visual photo-interpretation. In the experiment, a total of 59 circular 0.04-ha plots and 5294 trees were measured using STRS. The plots were investigated in the field and all STRS-trees and omission trees with a stem diameter of above 50 mm were mapped. The mapping was based on the use of the STRS-trees as geodetic control points. Redundant intertree azimuth and distance observations and a weighted least square adjustment of observations was used for the positioning of the omission trees. The commission error-rate was 2% in stem number and the omission trees constituted 10% of the total stem volume. Visual species recognition accuracy was 95% in classes of pine, spruce, broadleaved and dead trees. Height estimation accuracy of MSTM was 0.71 m or 4.7% in RMSE and it includes the DTM-errors. Stem diameter estimation RMSE was 29% and 20% when the crown widths were estimated using images and LiDAR, respectively. Underestimation of stem diameters was considerable, 3.4 and 1.0 cm. The inaccuracy of the stem diameter estimates degraded the accuracy of single-tree volume estimates and the results of estimating the proportion of assortments. Calibration of the STRS measurements and estimates are needed and this calls for field observations.

1. INTRODUCTION

1.1 Single-tree remote sensing from the viewpoint of forestry

The conventional way of measuring trees is giving way to new remote sensing applications, which have different scales of observation from individual trees to stands. Different sensors or methods that encompass certain levels of observation should not be taken as exclusionary alternatives. An optimal hybrid forest inventory most likely combines different data sources and furthermore, adjusts to the information needs that vary between stands and forest owners. Trees constitute a natural target of observation and single-tree remote sensing (STRS) aims at substituting the field measurements of position, species, height, stem diameter and volume. Preferably, a STRS-based forest inventory would be carried out without field visits, as it is largely based on direct measurements of the dimensions of the trees. However, STRS estimates seem to be prone to bias - e.g. the use of LiDAR often results in an underestimation of tree heights. This means that in situ data may be needed, at least for calibration.

The idea of photogrammetric STRS is old as early articles date back to the 1950s (e.g. Avery, 1958). Although the interest in the development has been extensive recently, especially in LiDAR-based methods (e.g. Persson et al. 2002), commercial STRS systems are essentially pending on the market. There are explicit difficulties to explain this. Scene complexity is an inherent aspect. Trees vary in crown size, shape and optical properties. Crowns are often interlaced. Occlusion and shading are present and result in omission errors. In boreal canopies, the trees with a relative height of above 0.5-0.7 are detectable in images and 0-12% of the total stem volume and nearly all short trees remain unseen (Korpela, 2004). The fact that small trees remain undetected is a serious shortage for many applications. The detectable trees constitute 90-100% of the commercial timber, which motivates for applications in timber cruising. Reliable species recognition is needed by foresters and remains currently unsolved. A satisfactory level of accuracy is above 95% (Korpela and Tokola, 2006). This can be very difficult to achieve in for example temperate forests, where several species of one family or genus coexist in a stand. Foresters are interested in the current and future properties of the stems and the information on available timber assortments in a given area. Improved decisions are made in silvicultural and logging operations based on this information. This pays for the data. The estimates need to be accurate enough and the expenses of data acquirement and analysis need to remain tolerable. Objectives that are set for STRS systems should reflect these information requirements.

1.2 Reducing the ill-posedness of STRS

Because of the complexity and ill-posed nature of optical and LiDAR-based STRS, it seems necessary to adopt the semi-automatic approach and to use auxiliary information about the targets. Allometry, the knowledge on the relative sizes of plant

parts, is used in STRS, when the measurements of species (*Sp*), height (*h*) and crown width (*dcrm*) are used for estimating the stem diameter (*dbh*) with allometric equations (e.g. Kalliovirta and Tokola, 2005). They are imperfect and the inaccuracy, approximately 10% for *dbh*, defines an upper limit of attainable accuracy. Allometry varies between species and between trees in a stand as trees adapt to the intra- and interspecific competition and site conditions. The functioning and structure of trees are closely linked and it might be possible to improve the estimation accuracy of *dbh*, if, STRS could provide accurate measurements of the foliage density, foliage mass (Ilomäki et al., 2004) or crown length (Kantola and Mäkelä, 2004). Another aspect of allometry is to use the regularities for designing filters of rational STRS observations and for finding gross errors. In model-based STRS, allometry can provide initial approximations of the model instances (e.g. Larsen and Rudemo, 1998). In our STRS-system, the semi-automatic approach and allometric knowledge are used in solving the tasks of STRS.

1.3 Objectives

A set of semi-automatic STRS methods that use multiple images and airborne LiDAR data were developed to form an entire STRS system (Figure 1).

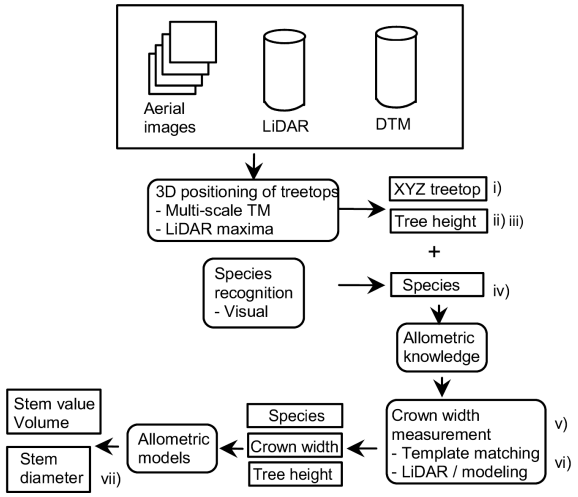

Figure 1. A schematic diagram of the STRS system with the data, tasks and output.

Allometric regularities are used for estimating the stem dimensions from STRS observations and for creating initial approximations of crown model instances. Following variables are measured by the system: i) Photogrammetric 3D treetop position using multi-scale template matching (MSTM), ii) photogrammetric tree height (*h_foto*) using the treetop position and a DTM, iii) LiDAR-based tree height (*h_LiDAR*), iv) species (*Sp_foto*) using visual image interpretation, v) image-based crown width (*dcrm_foto*) using MSTM, vi) LiDAR-based crown shape and width (*dcrm_LiDAR*) using least square adjustment of a crown model with the LiDAR point cloud and vii) stem diameter estimates (*dbh_foto*, *dbh_LiDAR*) using allometric equations. The system is described and a thorough performance test provided using a representative reference material from a systematic forest inventory. The rationales for our STRS system originate from the information needs in forestry and timber cruising in particular.

2. METHODS

2.1 Assumptions

It is assumed that multiple accurately oriented large-scale, >1:15000, aerial images and a semi-dense, 4-8 pulses per m^2, leaf-on LiDAR data are available. An accurate DTM is needed for reliable tree height estimation. Here, an experienced photo-interpreter performed the visual species recognition.

2.2 Semiautomatic photogrammetric 3D treetop positioning, height and crown width estimation using multi-scale template matching

Single-scale template matching has been successfully applied in 2D and 3D treetop estimation of regular stands, where crowns show only moderate variation (Pollock, 1996; Larsen and Rudemo, 1998; Korpela, 2004; 2007a). The semi-automatic method that was presented in Korpela (2004; 2007a) and uses a single template per an aerial image was modified towards a more manual and reliable method. Instead of trying to position all treetops in an area, which fails when trees exhibit variation, a method that utilizes multi-scale template matching (MSTM) and operator assistance was developed. In it, the templates representing crown instances in the different views are copied from the real aerial images by first manually measuring the 3D treetop position of a model tree. Model trees are needed for as many species as there are in the area of interest. In the images, elliptic templates are defined by 3 metric parameters and the templates capture the upper part of the crown (Korpela 2004 p. #). For MSTM, these sub-images are copied, low-pass filtered and scaled into N=11 scales between 0.5 and 1.2 using bilinear re-sampling. For K images, this results in N×K templates. The semi-automatic 3D treetop positioning follows. A treetop is pointed manually in an image that is preferred by the operator. This image observation defines a reference image-ray, which is sampled over a range in Z (Figure 2).

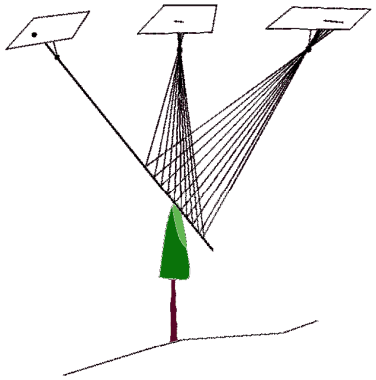

Figure 2. Illustration of the sampling of the reference image-ray over a search range in Z. The treetop position in the reference image is manually observed.

The search range in Z is one parameter that is set by the operator. It depends on the height variation of the trees and it is always centered on the Z of the previously measured treetop. At each 3D point along the reference image-ray, normalized cross-correlation (NCC) is computed in all images (along the epipolar lines) and templates (scales). The mean NCC of each scale is stored for each search point and the solution is the 3D point with the maximum NCC over all scales. Tree height (*h_foto*) is then given by the DTM by subtracting the terrain elevation from the elevation of the treetop.

Image-based crown width (*dcrm_foto*) estimation follows. The image with the smallest off-nadir angle is automatically selected for *dcrm_foto* estimation using MSTM. The 3D treetop position is mapped to this image and MSTM is tried in a small circular (r=0.4 m) image window near the projection point. The scale that gives the maximal NCC is used for the estimation of *dcrm_foto*: The crown width of the model tree, which is one of the 3 parameters that define the shape and position of the elliptic templates of the model tree, is multiplied by the scale factor to give *dcrm_foto* (Figure 3).

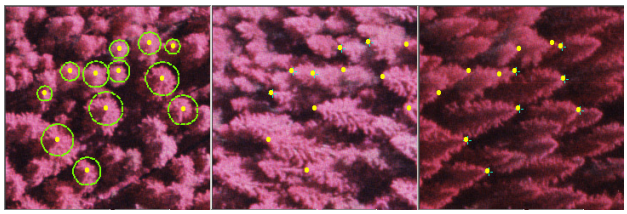

Figure 3. Results of MSTM in 3D treetop positioning and in *dcrm_foto* estimation: a CIR-image triplet of a pine-spruce stand. Solutions of twelve treetops are superimposed as yellow dots and the green circles depict estimates of *dcrm_foto*.

2.3 Species recognition

In tests with Vexcel Ultracam data (1:10000, GSD = 28 cm), it was found that the spectral values have considerable overlap between Scots pine, Norway spruce and birch. Within restricted areas in the front-lit parts of the images, the IR- and B-channels could potentially be used for species discrimination. The image-position seemed to cause variation in the spectral values. Also, young and old trees of the same species had varying spectral characteristics. The automatic approach was therefore discarded and visual interpretation of *Sp_foto* was applied. In an image set with 60% forward and side overlaps that was available here, there were always 1-2 views, where the crowns were seen back-lighted. These images are helpful for separating pine and spruce (Korpela et al., 2007). An experienced photo-interpreter carried out the visual interpretation.

2.4 Crown width estimation using LiDAR and least square adjustment of parametric crown models

A method was tried for LiDAR-based *dcrm* estimation, in which a parametric, non-linear crown model is iteratively fitted to the LiDAR point cloud (Figure 4; 5). The position and initial size and shape of the crown model are derived from the photogrammetric observations of *Sp_foto*, *h_foto* and the 3D treetop position. With these constraints, it was assumed that tree crown modeling is feasible even using rather a sparse LiDAR data. Crowns are approximated by a curve of revolution (1) that gives the crown radius $r(h_r)$ at a relative height $h_r \in [0..\pi/2]$ down from the treetop. The length of the crown is fixed to 40% of *h_foto*, which is a simplified approximation. The model is centered to the photogrammetric XYZ treetop position. If trees have only moderate slant, it can be assumed that the trunk is in the correct XY position. The crown model has three parameters and their initial values vary between species (Figure 4):

$$r(h_r) = a_1 \times h \times \sin(h_r)^{a_2} + a_3 \qquad (1)$$

Parameter a_1 sets the relationship between tree height and the maximum crown radius; a_2 is a shape parameter and a_3 gives the width of the top. If $a_3 \neq 0$, the top is flat. Using allometric data from the National Forest inventory of Finland (Kalliovirta and Tokola, 2005), conditional distributions of *dcrm* given *h* and *Sp* were derived. The relationship between *dcrm* and *h* was linear for all the three studied species: pine, spruce and birch. All broadleaved trees were treated as birches, as the proportion of other broadleaved trees is small in Finland. The conditional distributions were used in deriving initial values of parameter a_1. Initial values for parameter a_2 were set such that pine and spruce had a conical crown and birch a more round crown (Figure 4). At the start of the iteration, the crown instance was made to overestimate the expected crown envelope through a_1. Initial value of a_3 was 0.3 m for pine and spruce and 0.5 m for birch.

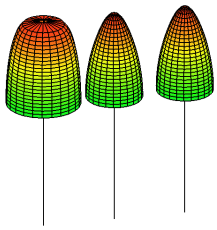

Figure 4. Illustration of three crown models for 22-m-high trees: a birch, a pine and a spruce. Birches have a 30-50% wider crown given the same tree height.

The LiDAR points that are inside the initial crown instance are collected and the relative height (h_r) down from the top and the XY distance (r) from the trunk is computed. These observations are used in solving a_1, a_2 and a_3 by a least square adjustment procedure. The highest DTM-normalized height of a LiDAR point alternatively inside the initial crown instance or inside a 0.6-m wide cylinder is stored and used as height estimate *h_LiDAR*. *dcrm_LiDAR* is given by the adjusted model.

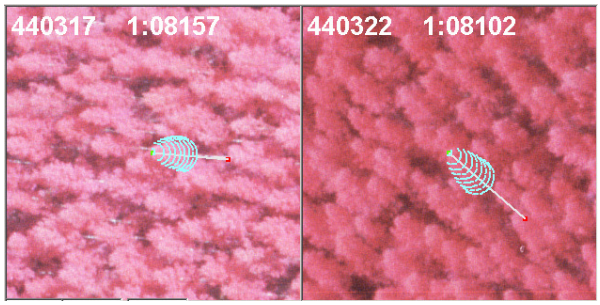

Figure 5. A view of an image pair after crown modeling of a birch. The "trunk" that is known from 3D treetop positioning is drawn in the images as well as the adjusted crown model. *dcrm_LiDAR* = 4.5 m, *h_foto* = 22.1 m and the RMSE of the model fit was 0.43 m. The texts give the image codes and the scale.

2.5 Allometric estimation of stem diameter and sortiment volumes

Equations by Kalliovirta and Tokola (2005) that predict *dbh* using *h* and *dcrm* for *Sp i* were applied:

$$\sqrt{dbh} = a_i \cdot \sqrt{h} + b_i \cdot \sqrt{dcrm} + \varepsilon_i \qquad (2)$$

The models (2) assume maximal *dcrm*. Here, *h_foto* was always used as the *h* estimate and *dbh* was computed alternatively with *dcrm_foto* or *dcrm_LiDAR* giving two estimates for each STRS-tree: *dbh_foto* and *dbh_LiDAR*. The first case represents a

situation, where no LiDAR data is available. Assessment of different assortments was made by simulating stem bucking into logs of saw wood and pulp wood. The calculation of tree and log volumes was done using polynomial stem taper curves by Laasasenaho (1982). They use *Sp*, *dbh* and *h* for predicting the stem form. The bucking algorithm used rules for allowable log lengths and the minimum top diameters.

3. EXPERIMENT

3.1 Study area, image and LiDAR data

The study site is a 56.8 ha forest in southern Finland (61°50' N, 24°20' E). The area consists of 25-70 and 100-130-yr-old stands. A systematic 50×50-m grid of 0.04-ha circular plots was established. Every 4th plot was selected and two additional plots giving a total of 59 plots and 2.36 ha (Figure 6). The image data is given in Table 1. Images were orientated in a hybrid bundle block adjustment (c.f. Korpela, 2006). For visual interpretation, the 5-channel Vexcel images were fused into CIR-images having a 9-cm GSD.

	Image set	
Date	July, 18 2004	August, 5 2006
Time	11:25	09:27
Scale	1:8000	1:10000
Overlaps	60/60%	60/30%
Sun elev.	45°	30°
Camera	RC30	UltraCam D
Focal lenght	0.214 m	0.105 m
Film-type	CIR Kodak 1443	PAN, R, G, G, IR
Film-size	23 × 23 cm	10 × 6 cm
GSD	12 cm	9 cm PAN, 28 cm MS

Table 1. Parameters of the two image sets.

A LiDAR-DTM was estimated using TerraModeler software from leaf-on data from August, 2004 having 0.7-2 points per m^2. Its accuracy was 0.27 m in a reference data of 8300 tacheometer points (Korpela and Välimäki, 2007). A semi-dense LiDAR from July 25, 2006 was available for tree crown modeling. An ALTM 3100 sensor with a pulse frequency of 100 kHz, a flying height of 800 m, a scan frequency of 70 Hz, a scan angle of ±14°, a flying speed of 75 m/s and strip overlaps of 55% were applied in the mission. The density of the data varies from 6 to 9 pulses per m^2 and from 1 to 4 points per pulse. The data had a minimum range difference of 3 m between points in a pulse. The footprint was approximately 25 cm.

3.2 STRS and field measurements

In April 2007, 5294 STRS-trees in the vicinity of the photo-plots were measured using the methods of sections 2.2-2.4. The work took 32 hours giving an average rate of 165 trees per hour. Each tree was measured for 3D treetop position, *h_foto*, *h_LiDAR*, *Sp_foto* and estimated for *dcrm_foto* and *dcrm_LiDAR*. From 3 to 6 images were used and the newest images from 2006 were included to reduce the underestimation of *h* caused by the 2-year mismatch of the 2004 images. There were always 6 images available on the computer screen for the visual species recognition into classes of pine, spruce, broadleaved and dead trees.

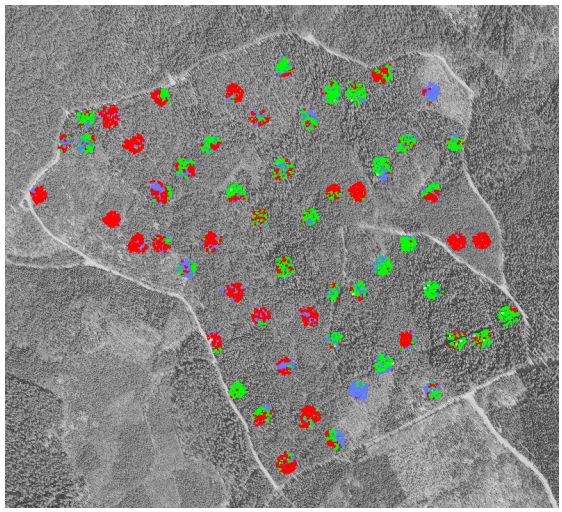

Figure 6. The 5294 STRS-treetops superimposed in a BW leaf-off topographic image from 1999. Forest roads define the borders of the 56.8-ha study area. The colors are: pine = red, spruce = green and broadleaved trees = blue.

The STRS-trees were processed into plot-wise maps (Figure 7). Labels to be fastened to the stems were printed. These had information of the STRS measurements and a map of the neighboring trees with azimuths as seen from the tree in question. A GPS-receiver with 1-m accuracy was used for finding the plot center. From then on, the field investigators used the map, intertree azimuths and a precision compass for identifying the STRS-trees. Cases, in which the STRS-tree did not have a unique counterpart in the field, the STRS-tree was made into a commission error. In addition to the STRS-trees, all omission trees with *dbh* of above 50 mm were mapped and included in the reference data and measured for *Sp* and *dbh* and assessed for the state of the crown. Every 3rd STRS-tree and every 6th omission tree were measured for *h* and crown length. The *h*-observations were done with a Suunto-hypsometer and the standard error (SE) was assumed to be 0.8 m. It undoubtedly varied between investigators, tree species and height classes.

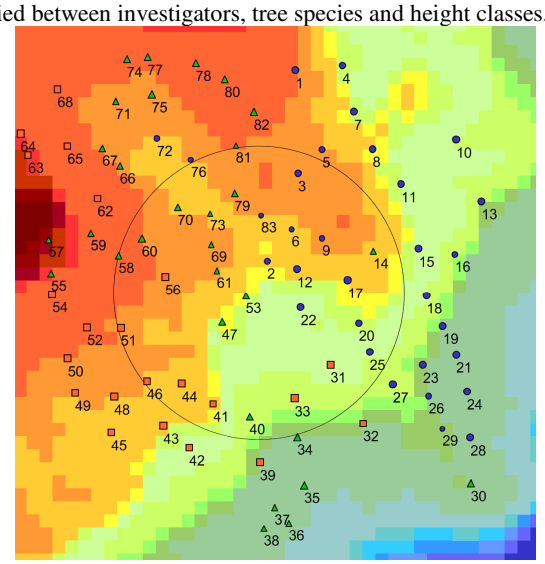

Figure 7. A tree map of STRS-trees that the investigators had in the field. The circle depicts the 0.04-ha plot and the STRS-trees are represented by species-specific symbols. A LiDAR-DTM in 1-m resolution is drawn in the background.

The mapping of the omission trees used a geodetic procedure, where the STRS-trees served the role of control points (Korpela et al., 2007). The investigators selected 3-4 STRS-trees with vertical stems and an unambiguous apex. These trunks were assumed to have an XY accuracy of 0.3 m. Intertree azimuths (spatial resection) were measured with a precision compass and intertree distances (trilateration) with a laser distance meter. Using weighted least square (WLS) adjustment of control point coordinates, intertree distances and azimuths, the omission trees were positioned with an average accuracy of 0.25 m in X and Y. The SE estimates of X and Y were above 0.75 m in 4 of 1410 omission trees. These trees had several gross observation errors and as the WLS adjustment could not be done in the field, it was arduous to track blunders. A leave-one-out technique was used to find cases with a single gross. Trees were also measured again.

3.3 Results - Performance of tree detection

2122 of 2205 STRS-trees were unambiguously found giving a commission error-rate of 3.7%. The commission error-rates were 1.8% for pine, 2.4% for spruce and 10.4% for the broadleaved trees.

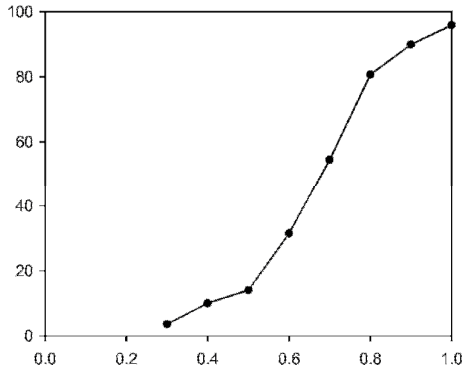

Figure 8. Results of tree detection. The curve gives the proportion (vertical axis, %) of correctly detected trees in 8 classes (0.3-1) of relative tree height.

Broadleaved trees can have round crowns, which affects the photogrammetric treetop positioning and makes the field identification of STRS-trees difficult. Broadleaved trees may have fused crowns, or the top of the crown consists of several upright thick branches, which are easily misinterpreted as individual trees. Commission errors were detected in 29/59 plots and the presence of broadleaved trees was associated with the number of commission errors. Since the detection of commission errors was a subjective process, it can be argued that a part of the commission errors were due to the prudence of the investigators. The true commission error-rate could only be examined by mapping the trees using tacheometry and by giving metric rules. From our field experience, we assumed that the true commission error-rate is approximately 2%. Omission trees constituted 38.8% of the stems (*dbh* > 50 mm) and 12% of the total stem volume. The omission error-rate in volume is thereby approximately 10%, if the "erroneous commission trees" are accounted for. (Figure 8).

3.4 Results - Species recognition

The species recognition accuracy was 93.7%, and if the 0-2% reference imprecision is accounted for, the accuracy is approximately 95% (Table 2).

Sp_foto	Field measured value				
	Pine	Spruce	Broadl.	Dead	All
Pine	**896**	37	8	6	947
Spruce	25	**726**	13	2	766
Broadl.	16	22	**354**	0	392
Dead	0	3	1	**4**	8
All	937	788	376	12	2113

Table 2. Error matrix of species recognition of the correctly found STRS-trees excluding 9 trees with tentative or missing reference measurements. Kappa = 0.90.

3.5 Results - Height estimation accuracy

The RMS-accuracy of *h_foto* was 0.71 m with an underestimation of 0.14 m (Table 3). Imprecision was largest in the broadleaved trees. Differences of up to 4 m were found. These may have resulted from errors in the 3D treetop positioning, the reference height observations or from errors in the DTM. *h_LiDAR* underestimated true *h* by 0.58 m (Table 4). The residuals of *h_foto* and *h_LiDAR* had an R^2 of 0.78. It is evident that a large part of the correlation is a result of the measurement errors in the field data. The underestimation of *h_LiDAR* was largest with spruce, which is explained by the peaked crown form.

Sp	N	Mean	SD	RMSE	RMSE-c
Pine	322	+0.17	0.93	0.94	0.50
Spruce	256	+0.19	1.07	1.08	0.73
Broadl.	128	–0.02	1.30	1.30	1.02
All	706	+0.14	1.06	1.07	0.71

Table 3. Accuracy of height estimates *h_foto* [m]. RMSE-c was calculated by subtracting the expected 0.8-m SE error of the field measurements from the observed RMSE. Mean reference *h* of all trees was 15.6 m.

Sp	N	Mean	SD	RMSE	RMSE-c
Pine	322	+0.58	0.88	1.05	0.69
Spruce	256	+0.69	1.01	1.22	0.92
Broadl.	128	+0.36	1.15	1.20	0.90
All	706	+0.58	0.99	1.14	0.82

Table 4. Accuracy of the height estimates *h_LiDAR* [m].

3.6 Results - Stem diameter estimation accuracy

The accuracy of *dbh_foto* estimates that were based on the use (2) of variables *Sp_foto*, *h_foto* and *dcrm_foto* was 28.7% in RMSE. The plot-level RMSEs were 15.8%-47.3%, which means that in the best cases the *dcrm-foto* measurement by MSTM had succeeded reasonably well. The 3.45-cm underestimation is most likely caused by the fact that the maximal crown width could not be seen in the images (Table 5). The estimates *dbh_LiDAR* that were predicted with models (2) using *Sp*, *h_foto* and *dcrm_LiDAR*, underestimated true *dbh* by 1 cm (Table 6). The overall RMSE was 19.6% with plot-level values ranging from 12.1% to 35.4%. The average *dcrm_foto* was 2.1 m, while the mean of *dcrm_LiDAR* was 2.9 m, which explains the differences in *dbh_foto* and *dbh_LiDAR*.

Sp	N	Mean	SD	RMSE
Pine	945	+3.96	3.33	5.17
Spruce	792	+3.24	3.08	4.47
Broadl.	376	+2.58	3.60	4.42
All	2113	+3.45	3.33	4.79

Table 5. Accuracy of stem diameter estimates *dbh_foto* [cm]. Mean diameter of all reference trees was 16.7 cm.

Sp	N	Mean	SD	RMSE
Pine	945	+0.73	3.12	3.21
Spruce	792	+1.39	2.99	3.30
Broadl.	376	+0.80	3.33	3.43
All	211	+0.99	3.13	3.28

Table 6. Accuracy of stem diameter estimates *dbh_LiDAR* [cm].

3.7 Results - Volume estimation accuracy

An RMSE of 60% was observed in the single tree volume estimates calculated with *dcrm_foto*. The plot-level RMSEs were 29.5%-108.1% (Table 6). The volume estimates that were based on the use of LiDAR in the estimation of crown width were more reliable. The RMSE for all trees was 46% and the plot-level RMSEs ranged from 24.6% to 101.4% (Table 7).

Sp	N	Mean	SD	RMSE
Pine	945	+82	102	131
Spruce	792	+74	107	130
Broadl.	376	+55	106	120
All	2113	+74	105	128

Table 6. Accuracy of single tree volume estimates [dm^3] calculated using *Sp*, *h_foto* and *dbh_foto* and the taper curves by Laasasenaho (1982). Mean reference volume was 214 dm^3.

Sp	N	Mean	SD	RMSE
Pine	945	+21	88	91
Spruce	792	+36	100	106
Broadl.	376	+24	94	98
All	2113	+28	94	98

Table 7. Accuracy of single tree volume estimates [dm^3] calculated using *Sp*, *h_foto* and *dbh_LiDAR*.

3.8 Results - STRS forest inventory

Variable	Inventory method		
	STRS		Field
Standing stems, n	53137	64.8 %	82042
Total volume, m^3	9783	80.8 %	12110
Saw wood, m^3	3522	67.6 %	5212
Pulp wood, m^3	5926	94.6 %	6264
Volume, Pine, m^3	4511	86.8 %	5198
Volume, Spruce, m^3	3919	73.0 %	5372
Volume Broadl., m^3	1262	80.9 %	1560

Table 8. Timber resources of the 56.8-ha forest with the STRS and field inventory. The STRS-results were computed using measurements of *Sp_foto*, *h_foto*, *dcrm_LiDAR* and *dbh_LiDAR*.

The timber resources were computed for the 56.8-ha forest using both STRS and the field measurements (Table 8). The STRS inventory lead to an underestimation of volume by 19.2%, which is explained by the omission errors (10 % in volume) and the 1-cm underestimation and 3-cm imprecision of the *dbh_LiDAR* estimates. An average STRS-tree had a *dbh* of 16.7 cm and an *h* of 15.6 m. A 1-cm underestimation in *dbh* for such a tree results in a 10-% underestimation of volume. The inaccuracy of the *dbh* estimates affected especially the accuracy of saw wood and pulp wood volume estimates. When the *dbh* of a single tree reaches 17-19 cm, the stem can be cut to provide a single log of saw wood, which constitutes 50% of the stem volume. Because *dbh_LiDAR* was biased and, above all, averaged due to regression modeling (2), saw wood volume was underestimated as much as 32.4%. Averaged *dbh* estimates induce systematic errors in the volume estimates, because the relationship between *dbh* and the volume is non-linear. Only 5% of the underestimation in saw wood volume was assessed to be due to omission errors, as the largest trees were measurable in the images (Figure 8). The rest of the underestimation, 27%, was due to the inaccuracy of *dbh_LiDAR*. Pulp wood volume was underestimated by only 5.4%. The seemingly good result is fallacious and a result of errors in stem bucking, which overestimated the proportion of pulp wood and underestimated the volume and number of saw wood logs because of the bias in *dbh_LiDAR*. Thereby, the results of Table 8 suggest strongly that a calibration of the STRS measurements and model estimates is required to avoid large systematic errors in the total estimates. The smaller underestimation in the volume of pine (13.2%) in comparison to spruce and the broadleaved trees is mainly explained by the differences in the relative height of the detected STRS-trees and the height variation of the species. Pine and Silver birch are light-demanding and spruce is a semi-shade-tolerant species. Also, the underestimation of *dbh_LiDAR* was largest for spruce.

4. DISCUSSION

The main result was that a STRS forest inventory was shown feasible, but that the results are subject to systematic errors that can only be eliminated with calibration. The STRS system provided the timber volume estimates per species and per sortiment, which is a must in a forest inventory. We demonstrated many difficulties that are inherent to STRS. Sampling, measurement and model errors all affected the results. Omission errors and biased measurements caused considerable systematic errors in the estimates of the timber resources. The use of the allometric regression models results in averaged *dbh* estimates even with error-free measurements. These, although free from systematic errors, resulted in biased volume estimates because of the non-linear dependencies. In all, the allometric estimation chain needs improvement.

The STRS measurements took 32 man-hours and the field work 500 with an extra 80 man-hours of data recording. The ratio was 1:18 between the two inventories. If larger photo-plots were used, less time per STRS-tree would have been needed, as the selection and measurement of the model tree in each plot was time-consuming. The costs should also include the image (~2€/ha) and LiDAR data (~3€/ha). Also, there was a high risk that no image data from 2006 was available because of bad weather. The weather risk is lesser with LiDAR and field work.

Multi-scale template matching (MSTM) was accurate in treetop positioning and *h* estimation. However, up to six large-scale images and an accurate LiDAR-DTM were available. The RMSE of *h* estimates was 0.5 m for pine, 0.7 m for spruce and 1.0 m for the broadleaved trees. The photogrammetric XY positioning accuracy was approximately 0.3 m, as the average σ_0 was close to 1, when a 0.3-m a priori SE was applied in the WLS-adjustment of photogrammetric coordinates, intertree azimuths (SE = 0.03 rad) and intertree distances (SE = 0.1 m) In all, the field mapping method of the omission trees, in which the STRS-trees were used as control points was satisfactory. In dense stands, where broadleaved trees formed the upper canopy, the mapping become tedious and subject to errors.

MSTM in near-nadir images for *dcrm* estimation resulted in badly biased *dbh* estimates with an RMSE of 29%. A plot-level RMSE of below 20% was observed in 7/59 plots. In first tests with the method (Korpela, 2007b), the accuracy of *dbh* estimates ranged from 16% to 21%, but the results were

obtained in well-structured stands and using images with a very low off-nadir angle. The technique needs further improvement. The use of synthetic templates should be tested (Larsen and Rudemo, 1998). The computation of NCC was done for gray-scaled versions of the images. Better results may be possible using a combination of channels. Also, the system could learn from good and compatible measurements, where the LiDAR-based estimates of *h* and *dcrm* are used to teach the system in the selection of better templates. The MSTM-based 3D treetop positioning algorithm was based on monoscopic observations by an operator and the process is slow. It might be possible to implement MSTM to find trees automatically. However, the very high computational costs of NCC need consideration. The 3D search space for photogrammetric treetop positioning is accurately known, if LiDAR data is available. This was not exploited here and the LiDAR data could be used more effective by using the monoplotting principle (e.g. Baltsavias, 1996). In it, LiDAR data would be processed into a canopy surface model to be intersected by the reference (treetop) images rays. The search space could then be adjusted to the height variation measured by the LiDAR (c.f. Korpela, 2007a).

The accuracy of the visual species recognition was 95% for classes of pine, spruce, broadleaved and dead trees. The achieved 95% classification accuracy is at the requisite level for Finnish forestry. However, in some areas a separation of the broadleaved trees at the species level would be needed. The automatic species recognition remains to be solved. Here, we see possibilities in the combined use of LiDAR and image data.

The crown modeling procedure with LiDAR needs further improvement, although it resulted in a *dbh* estimation accuracy of 20% with 14/59 plot-level RMSEs of below 15%. Avoiding LiDAR points of neighboring trees to affect the modeling might be possible by constructing geometric filters that take into account the spatial pattern of trees, which is partially known from photogrammetric 3D treetop positioning. This would mean that the LiDAR-based crown modeling is done only after the tree map is attained. The *dbh_LiDAR* underestimated true *dbh* by 1 cm, because the *dcrm* was not measured correctly by the crown model. The LiDAR pulses do not seek their way to the tips of the branches and when LS adjustment is applied, the extent of the crown envelope is inherently underestimated. The nominal density of the LiDAR data was 6-9 pulses per m^2 here - a lesser density may possibly suffice for crown modeling.

Generalization of the results requires care. Most trees had peaked and uniform crowns. One experienced photo-interpreter was tested. The orientation of the images was exact and the image sets had a faultless match. Also, the LiDAR from 2006 did not have XYZ offsets, which was examined using multi-temporal large-scale images. Using network-RTK, a height offset of 0.18 m was detected in the LiDAR-DTM from 2004 and corrected for. Performing such revisions is not feasible in practice. The stands were older than 25 years. In timber cruising young stands are less important, but in an inventory for forest management planning, they cannot be overlooked.

5. REFERENCES

Avery, G. 1958. Helicopter stereo-photography of forest plots. *Photogrammetric Engineering,* 24(4), pp. 617–624.

Baltsavias E., 1996. Digital ortho-images - A powerful tool for the extraction of spatial- and geo-information. *ISPRS JPRS,* 51(2), pp. 63-77.

Ilomäki, S., Nikinmaa, E. and Mäkelä, A., 2003. Crown rise due to competition drives biomass allocation in silver birch. *Canadian Journal of Forest Research,* 33(12), pp. 2395-2404.

Kalliovirta, J. and Tokola, T. 2005. Functions for estimating stem diameter and tree age using tree height, crown width and existing stand database information. *Silva Fennica,* 39(2), pp. 227-248.

Kantola, A, and Mäkelä, A., 2004. Crown development in Norway spruce [Picea abies (L.) Karst.]. *Trees - Structure and Function,* 18(4), pp. 408-421.

Korpela, I., 2004. Individual tree measurements by means of digital aerial photogrammetry. *Silva Fennica Monographs*, 3, pp. 1-93.

Korpela I., 2006. Geometrically accurate time series of archived aerial images and airborne lidar data in a forest environment. *Silva Fennica,* 40(1), pp. 109-126.

Korpela, I., 2007a. 3D treetop positioning by multiple image matching of aerial images in a 3D search volume bounded by lidar surface models. *PFG* 1/2007, pp. 35-44.

Korpela, I., 2007b. Incorporation of allometry into single-tree remote sensing with lidar and multiple aerial images. ISPRS Hannover Workshop, May 29-June 1, 2007. 6 p.

Korpela, I. and Tokola, T., 2006. Potential of aerial image-based monoscopic and multiview single-tree forest inventory - a simulation approach. *Forest Science*, 52(3), pp. 136-147.

Korpela, I. and Välimäki, E., 2007. Talousmetsän maanpintamallinnus arkistoilmakuvilta ja laserkeilauksella. [Terrain modeling using archived aerial images and airborne laser scanning]. Accepted in *Maanmittaus*.

Korpela, I., Tuomola, T. and Välimäki, E., 2007. Mapping forest plots: An efficient method combining photogrammetry and field triangulation. Accepted in *Silva Fennica*.

Laasasenaho, J., 1982. Taper curve and volume functions for pine, spruce and birch. *Communicationes Instituti Forestalis Fenniae,* 74. pp. 1-74.

Larsen, M. and Rudemo, M., 1998. Optimizing templates for finding trees in aerial photographs. *Pattern Recognition Letters* 19(12), pp. 1153–1162.

Persson, Å., Holmgren, J. and Söderman, U. 2002. Detecting and measuring individual trees using an airborne laser scanner. *PERS*, 68(9), pp. 925–932.

Pollock, R.J., 1996. The automatic recognition of individual trees in aerial images of forests based on a synthetic tree crown model. PhD-thesis in Computer Science. The University of British Columbia. 158 p.

ACKNOWLEDGEMENTS

We thank Professor Markus Holopainen for letting the study to be a part of the forest inventory course at the University of Helsinki. Our thanks are due to Timo Melkas and Reija Haapanen for helping us in the field.